Contribution from the Department of Chemistry,
Montana State University, Bozeman, Montana 59717

Nuclear Magnetic Resonance Investigation of the Formation of Oxalato, Malonato, and 2-Methylmalonato Complexes of Platinum(II). Crystal and Molecular Structures of Potassium *anti*-Bis(2-methylmalonato)platinate(II) Dihydrate and Potassium Dichloro(oxalato)platinate(II) Hydrate

S. O. Dunham, R. D. Larsen, and E. H. Abbott*

Received March 19, 1991

Nuclear magnetic resonance techniques utilizing ^{195}Pt and ^{13}C have been employed to study the formation of Pt(II) complexes of the dicarboxylic acids, oxalic (OxH_2), malonic ($MalH_2$), and 2-methylmalonic ($MmalH_2$) acid. Oxalic acid reacts with $K_2[PtCl_4]$ to form the monodentate $[Pt(OxH\text{-}O)Cl_3]^{2-}$, which reacts to form bidentate $[Pt(Ox)Cl_2]^{2-}$, then $[Pt(Ox)(OxH\text{-}O)Cl]^{2-}$ with one bidentate and one monodentate oxalato ligand, and, ultimately, the bis bidentate $[Pt(Ox)_2]^{2-}$. The structure of potassium dichloro(oxalato)platinate(II) hydrate has been determined by X-ray crystallography: $P\bar{1}$, a = 7.136 (2) Å, b = 7.308 (2) Å, c = 10.130 (4) Å, α = 86.75 (3)°, β = 74.58 (3)°, γ = 64.28 (2)°, V = 457.7 (3) Å^3, Z = 2, R = 0.0526, R_w = 0.0518. When the starting material is $[Pt(H_2O)_4]^{2+}$, similar complexes are observed. Analogous complexes are observed with both malonic and 2-methylmalonic acids. Monodentate malonato and 2-methylmalonato complexes are observed in solution and are more stable than monodentate oxalato complexes. Monodentate complexes are demonstrated by nonequivalence of their carboxylate and carboxylato ^{13}C resonances and by their chemical shifts in ^{195}Pt NMR spectra. Two ^{195}Pt resonances are observed for $[Pt(Mmal)(MmalH\text{-}O)Cl]^{2-}$, with one bidentate and one monodentate 2-methylmalonato ligand. Chirality at both α-carbon atoms results in two diastereomers of $[Pt(Mmal)(MmalH\text{-}O)Cl]^{2-}$. Separate ^{195}Pt resonances are observed for $[Pt(Mmal)_2]^{2-}$, in which methyl groups are syn or anti with respect to the Pt coordination plane. The structure of potassium *anti*-bis(2-methylmalonato)platinate(II) dihydrate has been determined by X-ray crystallography: $P\bar{1}$, a = 4.059 (1) Å, b = 9.107 (2) Å, c = 10.111 (2) Å, α = 98.49 (1)°, β = 101.28 (1)°, γ = 101.84 (1)°, V = 351.8 (1) Å, Z = 1, R = 0.0456, R_w = 0.0451.

Introduction

The solution coordination chemistry of platinum(II) complexes with multidentate ligands having both nitrogen and oxygen donor atoms has been well investigated.[1-11] Considerably less is known about multidentate ligand complexes with only oxygen donors. The bis(oxalato)platinate(II) complex was identified over a century ago and has been well characterized.[12-16] The extensions to bis(malonato), -(squarato), and -(acetylacetonato) complexes have been described only recently.[17-20] Complexes of platinum(II) with bidentate oxygen donors have generated considerable interest in several areas. Partially oxidized polymers of bis(oxalato)platinate(II) are one-dimensional conductors.[21] A new generation of antitumor drugs is based on mixed-ligand complexes involving a *cis*-diammineplatinum(II) fragment and various bidentate oxygen donor ligands.[1,2,22,23]

It is well established that ^{195}Pt NMR spectroscopy is a valuable method for structure elucidation and determination of reaction mechanisms of platinum complexes.[1-11,24-32] ^{195}Pt NMR studies of amino acid complexes of *cis*-$[Pt(NH_3)_2(H_2O)_2]^{2+}$ have shown that unidentate O-bound ligands can have a long lifetime before ring closure to form a N,O-chelate ring.[3-11] However, recent reports of the reaction between *cis*-$[Pt(NH_3)_2(H_2O)_2]^{2+}$ and 2-aminomalonic acid studied by ^{195}Pt NMR spectroscopy indicate that monodentate O-bound species are not observed enroute to the bidentate metastable O,O′-bound 2-aminomalonato complex.[1,2]

In the present work, multinuclear NMR spectroscopy and X-ray crystallography are used to demonstrate the structure of complexes formed between platinum(II) and multidentate oxygen donor ligands. Chelated complexes are the eventual products, but monodentate complexes are present in high concentrations during ligand substitution reactions and in low concentrations at equilibrium. Monodentate complexes could have considerable importance in the substitution reactions of platinum(II) and should be considered in assessing the biological activity of new-generation antitumor drugs.[22,23,33-36]

Experimental Section

Starting Materials. Oxalic (OxH_2), malonic ($MalH_2$), and 2-methylmalonic acids ($MmalH_2$) (Aldrich) and $K_2[PtCl_4]$ (**1**) (Johnson Matthey) were used as supplied. $[Pt(H_2O)_4]^{2+}$ (**6**) was prepared as previously described.[37]

(1) Appleton, T. G.; Hall, J. R.; Neale, D. W.; Thompson, C. S. M. *Inorg. Chem.* **1990**, *29*, 3985.
(2) Gibson, D.; Rosenfeld, A.; Apfelbaum, H. C.; Blum, J. *Inorg. Chem.* **1990**, *29*, 5125.
(3) Appleton, T. G.; Hall, J. R.; Hambley, T. W.; Prenzler, P. D. *Inorg. Chem.* **1990**, *29*, 3562.
(4) Schwederski, B. E.; Lee, J. D.; Margerum, D. W. *Inorg. Chem.* **1990**, *29*, 3569.
(5) Appleton, T. G.; Hall, J. R.; Prenzler, P. *Inorg. Chem.* **1989**, *28*, 815.
(6) Appleton, T. G.; Hall, J. R.; McMahon, I. *Inorg. Chem.* **1986**, *25*, 720.
(7) Appleton, T. G.; Hall, J. R.; McMahon, I. *Inorg. Chem.* **1986**, *25*, 726.
(8) Appleton, T. G.; Hall, J. R.; Ralph, S. F. *Aust. J. Chem.* **1986**, *39*, 1347.
(9) Appleton, T. G.; Berry, R. D.; Hall, J. R. *Inorg. Chem.* **1985**, *24*, 666.
(10) Appleton, T. G.; Hall, J. R.; Ralph, S. F. *Inorg. Chem.* **1985**, *24*, 673.
(11) Appleton, T. G.; Hall, J. R. *J. Chem. Soc., Chem. Commun.* **1983**, 911.
(12) Soderbaum, H. G. *Bull. Soc. Chim. Fr.* **1886**, *45*, 188.
(13) Krogmann, K.; Dodel, P. *Chem. Ber.* **1966**, *99*, 3402.
(14) Krogmann, K.; Dodel, P. *Chem. Ber.* **1966**, *99*, 3408.
(15) Mattes, V. R.; Krogmann, K. *Z. Anorg. Allg. Chem.* **1964**, *332*, 247.
(16) Rimkus, V. G.; Preetz, W. *Z. Anorg. Allg. Chem.* **1983**, 73.
(17) Grabowski, A.; Preetz, W. *Z. Anorg. Allg. Chem.* **1987**, 101.
(18) Toftlund, H. *J. Chem. Soc., Chem. Commun.* **1979**, 837.
(19) Simonsen, O.; Toftlund, H. *Inorg. Chem.* **1981**, *20*, 4044.
(20) Katoh, M.; Miki, K.; Kai, Y.; Tanaka, N.; Kasai, N. *Bull. Chem. Soc. Jpn.* **1981**, *54*, 611.
(21) Miller, J. S.; Epstein, A. J. *Prog. Inorg. Chem.* **1976**, *20*, 1 and references therein.
(22) Bitha, P.; Morton, G. O.; Dunne, T. S.; Delos Santos, E. F.; Lin, Y.; Boone, S. R.; Haltiwanger, R. C.; Pierpont, C. G. *Inorg. Chem.* **1990**, *29*, 645.
(23) Bruck, M. A.; Bau, R.; Noji, M.; Inagaki, K.; Kidani, Y. *Inorg. Chim. Acta* **1984**, *92*, 279.
(24) Wu, L.; Schwederski, E.; Margerum, D. W. *Inorg. Chem.* **1990**, *29*, 3578.
(25) Groning, O.; Elding, L. I. *Inorg. Chem.* **1989**, *28*, 3366.
(26) Gill, D. S.; Rosenberg, B. *J. Am. Chem. Soc.* **1982**, *104*, 4598.
(27) Groning, O.; Drakenberg, T.; Elding, L. I. *Inorg. Chem.* **1982**, *21*, 1820.
(28) Appleton, T. G.; Connor, J. W.; Hall, J. R. *Inorg. Chem.* **1988**, *27*, 130.
(29) Appleton, T. G.; Hall, J. R.; Ralph, S. F.; Thompson, C. S. M. *Inorg. Chem.* **1984**, *23*, 3421.
(30) Appleton, T. G.; Connor, J. W.; Hall, J. R.; Prenzler, P. *Inorg. Chem.* **1989**, *28*, 2030.
(31) Appleton, T. G.; Hall, J. R.; Ralph, S. F.; Thompson, C. S. *Inorg. Chem.* **1989**, *28*, 1989.
(32) Appleton, T. G.; Berry, R. D.; Davis, C. A.; Hall, J. R.; Kimlin, H. A. *Inorg. Chem.* **1984**, *23*, 3514.
(33) Teggins, J. E.; Milburn, R. M. *Inorg. Chem.* **1964**, *3*, 364.
(34) Teggins, J. E.; Milburn, R. M. *Inorg. Chem.* **1965**, *4*, 793.
(35) Giacomelli, A.; Indelli, A. *Inorg. Chem.* **1972**, *11*, 1033.
(36) Hoch, J.; Milburn, R. M. *Inorg. Chem.* **1977**, *18*, 886.

0020-1669/91/1330-4328$02.50/0

Potassium Bis(oxalato)platinate(II) (5). The complex was prepared by the method of Krogmann and Dodel from $K_2[PtCl_4]$ (**1**).[13]

Preparations. Potassium Dichloro(oxalato)platinate(II) (3). $K_2[Pt(Ox)_2]\cdot 2H_2O$ (**5**) (0.050 g, 0.103 mmol) was dissolved in 3 mL of H_2O. Ten equivalents of KCl (0.077 g, 1.03 mmol) was added as a solid and the solution heated at 50 °C for 24 h. ^{195}Pt NMR spectroscopy shows the predominant species to be **3** with less than 10% contribution from **1** and **5**. The solution was cooled to 5 °C and centrifuged to separate precipitated **5**. Vapor diffusion of acetone into the supernate produced clear and red crystals. The clear crystals were presumed to be KCl and were not investigated. A red crystal was selected and mounted for X-ray diffraction.

Potassium and Sodium Bis(malonato)platinates(II) (13). Malonic acid (0.50 g, 4.8 mmol) was dissolved in 25 mL of water. The pH of the solution was adjusted with 3 M KOH to 6.0. $K_2[PtCl_4]$ (**1**) (0.200 g, 0.48 mmol) was added as a solid and the solution stirred for 3 days at room temperature, during which time ^{195}Pt NMR spectroscopy was used to follow the concentration of species in solution. The yellow solution was rotary-evaporated to near dryness and the solid dissolved in a minimum amount of warm water. The solution was left overnight in a refrigerator at 5 °C, and the solid was centrifuged from the supernate. The solid was washed twice with 1 mL of cold water. Repeated stirring and concentration of the supernate gave 75% yield (0.184 g). The preparation of the sodium salt was the same as for the potassium salt, except the malonic acid solution was neutralized with 3 M NaOH. The sodium salt is less soluble than the potassium salt.

Potassium and Sodium *syn*- and *anti*-Bis(2-methylmalonato)platinates(II) (22, 23). The potassium and sodium salts were prepared by the same procedure as for the malonato complex (86% yield). Sodium salts are less soluble than potassium salts. The syn and anti isomers can be separated from each other by their solubility in H_2O. When the yellow solid obtained from concentrating and cooling to 5 °C was washed with cold water, the supernate was enriched in the syn isomer **22**. Dissolving both isomers in a minimum amount of warm water and then storing overnight at 5 °C yielded predominantly the anti isomer **23** as a yellow solid. Vapor diffusion of acetone into an aqueous solution of the yellow solid gave yellow/green needles that were used for X-ray diffraction.

Tetra-*n*-butylammonium Salts. These compounds were prepared as previously described.[16,17] The solids obtained are soluble in dichloromethane, methanol, ethanol, and chloroform.

NMR Spectroscopy. ^{195}Pt spectra were recorded at 53.52 and 107.47 MHz, and ^{13}C spectra were recorded at 62.89, 75.46, and 125.76 MHz on Bruker WM250, AC300, and AM500 spectrometers. ^{195}Pt spectra were typically run at 50 000-Hz spectral width, with 16 000 scans, 4K data points, and 0.04 s between 30-μs pulses (50° tilt). Chemical shifts were measured relative to an external standard of 0.1 M $Na_2[PtCl_6]$ = 0 ppm. Integratable spectra were run at 10 000-Hz width, with 4000 scans, 4K data points, and 0.5 s between 30-μs pulses. ^{13}C and ^1H spectra were corrected to TMS with internal references of dioxane (^{13}C = 67.73 ppm, ^1H = 3.53 ppm) in water or $CDCl_3$ (^{13}C = 77.0 ppm, ^1H = 7.24 ppm) in chloroform.

Reactions with $[PtCl_4]^{2-}$ (**1**) were studied as follows. Approximately 0.050 g of **1** was dissolved in 1.5 mL of H_2O. The solution was centrifuged, and the supernate was placed in a 10-mm NMR tube. Ten mole equivalents of ligand dissolved in 1.4 mL of H_2O was added to the solution of **1**. A 0.1-mL portion of D_2O was added for a lock signal. The pH of the solution was adjusted with 3 M KOH or NaOH. To follow the reaction of $[Pt(H_2O)_4]^{2+}$ (**6**) with one of the ligands, approximately 20 mL of a stock solution of **6** in 1 M $HClO_4$ (2.5 mg/mL) was precipitated as $[Pt(OH)_2]\cdot nH_2O$ at pH 7.0 by addition of NaOH.[37] The solid $[Pt(OH)_2]\cdot nH_2O$ was filtered off, washed with 3 mL of cold water, and immediately dissolved in 2.9 mL of H_2O containing 0.1 mL of D_2O and 10 mol equiv of the acid form of the ligand. ^{195}Pt NMR spectroscopy showed only a single resonance for **6** when $[Pt(OH)_2]\cdot nH_2O$ solid dissolved. The solution/suspension was degassed by freeze-thawing and flushing with argon five times in a 10-mm NMR tube fitted with a rubber septum. Undissolved $[Pt(OH)_2]\cdot nH_2O$ slowly dissolved as the reaction progressed. These solutions were stable for at least 3 weeks, after which dark blue/black solutions were observed owing to oxidation of platinum complexes. Solutions that were not degassed turned dark blue/black as complexes were formed.

Structure Determinations and Refinements. $K_2[Pt(C_2O_4)Cl_2]\cdot H_2O$ (3). A thin plate-shaped red crystal (approximately 0.04 × 0.13 × 0.30 mm) was mounted on a glass fiber for crystallographic data collection. Unit cell dimensions were obtained by least-squares refinement using 25 centered reflections for which 18° < 2θ < 26° (graphite-monochromatized Mo Kα radiation). Intensity data ($\pm h,\pm k,+l$) were taken on a Nicolet R3mE four-circle diffractometer. Due to gradual loss of beam intensity from a weak X-ray tube, the three check reflections, monitored every 100 reflections, showed approximately 37% loss of intensity during the course of data collection. Since the loss of intensity for the check reflections followed a smooth curve, intensity data were scaled from that curve. Crystallographic data for this compound appear in Table I.

Table I. Crystallographic Data

Potassium Dichloro(oxalato)platinate(II) Hydrate, $K_2[Pt(C_2O_4)Cl_2]\cdot H_2O$	
a = 7.136 (2) Å	fw = 450.25
b = 7.308 (2) Å	space group $P\bar{1}$
c = 10.130 (4) Å	T = 24 °C
α = 86.75 (3)°	λ = 0.71069 Å (Mo Kα)
β = 74.58 (3)°	ρ_{calcd} = 3.27 g cm^{-3}
γ = 64.28 (2)°	μ = 169.6 cm^{-1} (Mo Kα)
V = 457.7 (3) Å^3	transm factor range = 0.10–0.49
Z = 2	$R_w(F_o)$ = 0.0518
$R(F_o)$ = 0.0526	
Potassium *anti*-Bis(2-methylmalonato)platinate(II) Dihydrate, $K_2[anti\text{-}Pt(C_4H_4O_4)_2]\cdot 2H_2O$	
a = 4.059 (1) Å	fw = 541.5
b = 9.107 (2) Å	space group $P\bar{1}$
c = 10.111 (2) Å	T = 24 °C
α = 98.49 (1)°	λ = 0.71069 Å (Mo Kα)
β = 101.28 (1)°	ρ_{calcd} = 2.56 g cm^{-3}
γ = 101.84 (1)°	μ = 107.1 cm^{-1} (Mo Kα)
V = 351.8 (1) Å^3	transm factor range = 0.14–0.43
Z = 1	$R_w(F_o)$ = 0.0451
$R(F_o)$ = 0.0456	

Data reduction,[38] including corrections for Lorentz and polarization effects, gave 3994 independent reflections in the range 4° < 2θ < 70°, of which 1985 with $I > 3\sigma(I)$ were used for structure refinement. The volume of the triclinic unit cell was appropriate for two formula units so the centric space group was assumed and later confirmed by successful structure solution and refinement. The platinum position was determined from a Patterson synthesis, and remaining non-hydrogen positions were determined by difference synthesis.

$K_2[anti\text{-}Pt(C_4O_4H_4)_2]\cdot 2H_2O$ (23). A yellow/green needle-shaped crystal (approximately 0.08 × 0.11 × 0.28 mm) was mounted on a glass fiber. Unit cell dimensions were obtained by least-squares refinement using 25 centered reflections for which 20° < 2θ < 30°. Three check reflections, monitored every 100 reflections, showed approximately 5% loss of intensity during the course of data collection, and intensity data were scaled accordingly. Crystallographic data for this compound appear in Table I. Data reduction gave 4806 unique reflections in the range 4° < 2θ < 83°, of which 3616 with $I > 3\sigma(I)$ were used for structure refinement. The volume of the triclinic unit cell was appropriate for one formula unit. A Patterson synthesis did not reveal any nonorigin peak of sufficient magnitude for a platinum–platinum vector, confirming the indication from the unit cell volume. Placement of the platinum atom on the inversion center in the centric space group led to successful structure solution and refinement. The remaining positions of the chelate ring were located from difference synthesis.

For both structures all non-hydrogen atoms were refined anisotropically by block-cascade least-squares minimizing $\sum w\Delta^2$. The weighting scheme used was $w = k(\sigma^2(F_o) + 0.001F_o^2)^{-1}$. Absorption corrections were calculated by Gaussian integration using crystal dimensions between indexed crystal faces. Atomic scattering factors, including terms for anomalous scattering, were taken from ref 39. Calculated hydrogen positions with a refined isotropic thermal parameter were used, with the orientation of the methyl group in **23** determined from a difference map. Water hydrogens were not included. Five reflections in the data sets for each compound showed significant extinction and were excluded during final refinements. Neither refinement converged in the acentric space group. Final difference maps showed only the usual ripple near the platinum positions. Atom coordinates are given in Tables II and III.

Results and Discussion

Nuclear Magnetic Resonance Studies. Two principles were used extensively in assigning the observed NMR resonances: (1) For

(37) Elding, L. I. *Inorg. Chim. Acta* **1976**, *20*, 65.

(38) All crystallographic calculations were performed on a Data General Eclipse computer using a SHELXTL program package by G. M. Sheldrick, Nicolet Instrument Corp., Madison, WI.

(39) Cromer, D. T.; Waber, J. T. *International Tables for X-ray Crystallography*; Kynoch: Birmingham, England, 1974; Vol. IV, pp 72–98, 149–150.

Table II. $K_2[Pt(C_2O_4)Cl_2]\cdot H_2O$: Atomic Coordinates and Equivalent Isotropic Temperature Factors (Å²) with Standard Deviations

atom	x/a	y/b	z/c	U_{eq}[a]
Pt	0.5230 (1)	0.2449 (1)	0.4452 (1)	0.0221 (2)
Cl(1)	0.3486 (6)	0.3917 (6)	0.2790 (4)	0.037 (2)
Cl(2)	0.8435 (5)	0.0581 (6)	0.2870 (4)	0.034 (1)
O(1)	0.251 (2)	0.394 (2)	0.598 (1)	0.030 (4)
O(2)	0.652 (2)	0.129 (2)	0.606 (1)	0.027 (4)
C(1)	0.279 (2)	0.356 (2)	0.718 (1)	0.024 (5)
C(2)	0.511 (2)	0.187 (2)	0.722 (2)	0.025 (5)
O(3)	0.144 (2)	0.436 (2)	0.826 (1)	0.045 (5)
O(4)	0.545 (2)	0.119 (2)	0.831 (1)	0.040 (5)
K(1)[b]	0.9967 (4)	−0.2492 (4)	0.5096 (4)	0.031 (1)
K(2)[b]	0.1612 (6)	0.1860 (6)	0.0451 (4)	0.049 (2)
O(5)[b]	0.229 (2)	−0.251 (3)	0.011 (2)	0.08 (1)

[a] Equivalent isotropic U defined as one-third of the trace of the orthogonalized U_{ij} tensor. [b] Potassium ions and the water oxygen atom are not shown in Figure 5.

Table III. $K_2[anti\text{-}Pt(C_4H_4O_4)_2]\cdot 2H_2O$: Atomic Coordinates and Equivalent Anisotropic Temperature Factors (Å²) with Standard Deviations

atom	x/a	y/b	z/c	U_{eq}[a]
Pt	0.00000	0.00000	0.00000	0.0177 (1)
O(1)	0.096 (1)	−0.2077 (4)	0.0023 (4)	0.026 (1)
O(2)	0.172 (1)	0.0182 (4)	−0.1706 (4)	0.027 (1)
C(1)	0.096 (1)	−0.2969 (5)	−0.1108 (5)	0.023 (1)
C(2)	−0.050 (1)	−0.2562 (5)	−0.2470 (5)	0.023 (1)
C(3)	0.154 (1)	−0.1000 (5)	−0.2619 (5)	0.022 (1)
C(4)	−0.086 (2)	−0.3806 (7)	−0.3702 (6)	0.036 (2)
O(3)	0.211 (2)	−0.4116 (5)	−0.1073 (5)	0.040 (2)
O(4)	0.299 (1)	−0.0897 (5)	−0.3573 (5)	0.036 (1)
K(1)[b]	0.3638 (4)	0.3189 (1)	0.8291 (1)	0.0310 (3)
O(5)[b]	0.302 (1)	−0.2051 (6)	−0.6369 (5)	0.040 (2)

[a] Equivalent isotropic U defined as one-third of the trace of the orthogonalized U_{ij} tensor. [b] Potassium ions and water oxygen atoms are not shown in Figure 6.

monodentate complexes, ^{195}Pt shifts depend in a additive way on the nature of the donor atom.[40] (2) When five- and six-membered bidentate chelate rings are formed between given donor atoms, large upfield shifts are observed.[1,2,4,41,42] A summary of all chemical shift data appears in Tables IV and V.

Oxalate Reactions. When oxalic acid is added to a solution of $[PtCl_4]^{2-}$ (**1**), new resonances appear at −1167 and −1005 ppm, downfield from the starting material. The resonance at −1167 ppm is 18 ppm from $[PtCl_3(H_2O)]^-$[29] and is assigned to $[Pt(OxH\text{-}O)Cl_3]^{2-}$ (**2**), in which oxalate is monodentate. The peak at −1005 ppm is larger and is assigned to $[Pt(Ox)Cl_2]^{2-}$ (**3**), in which oxalate is bidentate. It falls 194 ppm to higher field than the peak for *cis*-$[PtCl_2(H_2O)_2]$,[27] in keeping with the large upfield shift observed upon formation of five- and six-membered bidentate chelate rings. The carboxylate group for **3** is a single ^{13}C resonance at 170.12 ppm. The structure was confirmed by X-ray crystallography; vide infra. At pH 2.0, these are the only resonances observed except those for the hydrolysis products of **1**.

When the pH is raised above 3.0, new ^{195}Pt resonances are observed at −620 and −525 ppm before a yellow/green solid begins to precipitate. The solid was recrystallized from warm water to yield $K_2[Pt(Ox)_2]\cdot 2H_2O$ (**5**), which is identified from its unit cell.[15] For **5**, a single ^{13}C resonance is observed at 170.2 ppm and a single ^{195}Pt resonance is observed at −525 ppm. The ^{195}Pt resonance for **5** is 560 ppm upfield from that of $[Pt(H_2O)_4]^{2+}$ (**6**), again demonstrating the additive large upfield shift observed for bidentate chelate ring formations. The resonance at −625 ppm arises from a transitory species formed as **3** is converted to **5**. Its low concentration prevented ^{13}C NMR data collection. Its ^{195}Pt resonance is 384 ppm downfield from **3** and could be consistent with either of two complexes. The first is formed by replacement of chloride with an oxygen donor, and the second is the formation of a binuclear bridged μ-chloro or μ-hydroxo chloro species. However, a bridged species should not be favored in this pH range.[31] We favor the formulation $[Pt(Ox)(OxH\text{-}O)Cl]^{2-}$ (**4**), where one oxalate is monodentate and the other oxalate is a bidentate ligand. When KCl is added to a solution of **5** at pH 5.0, ^{195}Pt NMR spectroscopy shows the predominant species to be **3** and **1**. The intermediate complexes **2** and **4** are not observed in this pH range because of the fast chelate ring closure of deprotonated oxalate ligand. We find no evidence for the *trans*-$[Pt(OxH\text{-}O)_2Cl_2]^{2-}$ species proposed by Hoch and Milburn.[36] It would appear that the intermediate species they observed was indeed **3** and that the chelate effect dominates the trans effect of chloride in these Pt(II) complexes.

Table IV. ^{195}Pt NMR Data

complex[a]	struct no.	δ
$[PtCl_4]^{2-}$[b]	**1**	−1624
$[Pt(H_2O)_4]^{2+}$[b]	**6**	24
$[Pt(OxH\text{-}O)Cl_3]^{2-}$	**2**	−1167
$[Pt(Ox)Cl_2]^{2-}$	**3**	−1005
$[Pt(Ox)(OxH\text{-}O)Cl]^{2-}$	**4**	−620
$[Pt(Ox)_2]^{2-}$	**5**	−525
$[Pt(OxH\text{-}O)(H_2O)_3]^+$	**7**	−24
$[Pt(Ox)(H_2O)_2]$	**8**	−338
$[Pt(Ox)(OxH\text{-}O)(H_2O)]^-$	**9**	−345
$[Pt(MalH\text{-}O)Cl_3]^{2-}$	**10**	−1149
$[Pt(Mal)Cl_2]^{2-}$	**11**	−978
$[Pt(Mal)(MalH\text{-}O)Cl]^{2-}$	**12**	−595
$[Pt(Mal)_2]^{2-}$	**13**	−562
$[Pt(MalH\text{-}O)(H_2O)_3]^+$	**14**	−32
$[Pt(MalH\text{-}O)_2(H_2O)_2]$	**15**	−74
$[Pt(Mal)(H_2O)_2]$	**16**	−314
$[Pt(Mal)(MalH\text{-}O)(H_2O)]^-$	**17**	−331
$[Pt(MmalH\text{-}O)Cl_3]^{2-}$	**18**	−1149
$[Pt(Mmal)Cl_2]^{2-}$	**19**	−995
$[Pt(Mmal)(MmalH\text{-}O)Cl]^{2-}$	**20**	−623
$[Pt(Mmal)(MmalH\text{-}O)Cl]^{2-}$	**21**	−623
$[Pt(Mmal)_2]^{2-}$[c]	**22**	−608
$[Pt(Mmal)_2]^{2-}$[d]	**23**	−600
$[Pt(MmalH\text{-}O)(H_2O)_3]^+$	**24**	−34
$[Pt(MmalH\text{-}O)_2(H_2O)_2]$	**25**	−78
$[Pt(Mmal)(H_2O)_2]$	**26**	−339
$[Pt(Mmal)(MmalH\text{-}O)(H_2O)]^-$	**27**	−356

[a] Ox = oxalato, Mal = malonato, Mmal = 2-methylmalonato. [b] Chemical shifts reported in ref 29. [c] Methyl groups syn. [d] Methyl groups anti.

Table V. ^{13}C NMR Data

complex	struct no.	δ carboxyl	δ methylene	δ methyl
$[Pt(Ox)Cl_2]^{2-}$	**3**	170.12		
$[Pt(Ox)Cl_2]^{2-}$[a]	**3**	168.02		
$[Pt(Ox)_2]^{2-}$	**5**	170.20		
$[Pt(Ox)_2]^{2-}$[a]	**5**	168.39		
$[Pt(Mal)Cl_2]^{2-}$	**11**	179.47	49.24	
$[Pt(Mal)(MalH\text{-}O)Cl]^{2-}$	**12**	180.14		
		179.72		
		179.42		
		177.08		
$[Pt(Mal)_2]^{2-}$	**13**	180.36	48.31	
$[Pt(Mal)_2]^{2-}$[a]	**13**	177.19	49.89	
$[Pt(MalH\text{-}O)(H_2O)_3]^+$	**14**	178.70		
		173.36		
$[Pt(Mal)(H_2O)_2]$	**16**	180.37	48.84	
$[Pt(Mmal)Cl_2]^{2-}$	**19**	181.43	52.05	14.49
$[Pt(Mmal)_2]^{2-}$	**22**	182.34	51.79	14.57
$[Pt(Mmal)_2]^{2-}$	**23**	182.43	51.92	14.69
$[Pt(Mmal)_2]^{2-}$[a]	**22**	178.98	51.39	14.60
$[Pt(Mmal)_2]^{2-}$[a]	**23**	179.17	51.21	14.47
$[Pt(MmalH\text{-}O)(H_2O)_3]^+$	**24**	176.65	47.51	14.65
$[Pt(Mmal)(H_2O)_2]$	**26**	182.18	51.61	14.97

[a] Tetra-*n*-butylammonium salts in $CDCl_3$.

(40) Kerrison, S. J. S.; Sadler, P. J. *J. Magn. Reson.* **1978**, *31*, 321.
(41) Bowler, B. E.; Ahmed, K. J.; Sundquist, W. I.; Hollis, L. S.; Whang, E. E.; Lippard, S. J. *J. Am. Chem. Soc.* **1989**, *111*, 1299.
(42) Neidle, S.; Ismail, I. M.; Sadler, P. J. *J. Inorg. Biochem.* **1980**, *13*, 205.

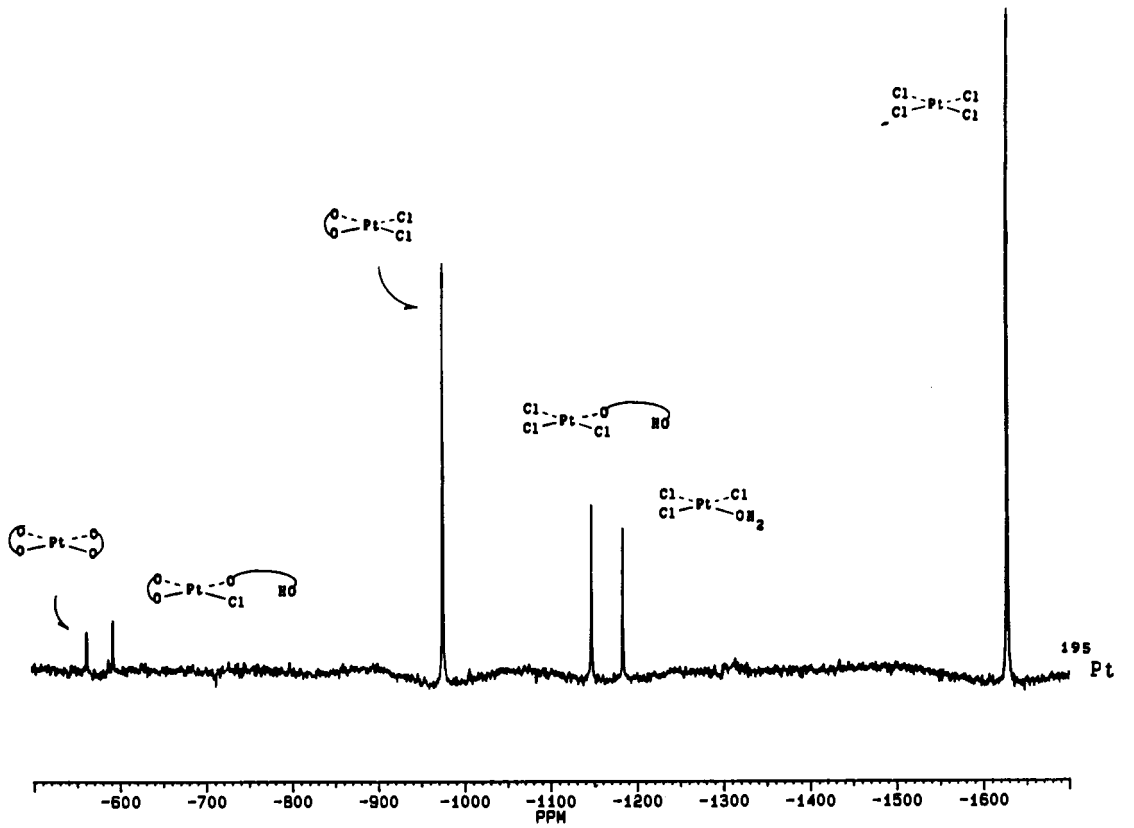

Figure 1. ^{195}Pt NMR spectrum of the reaction of malonic acid with $K_2[PtCl_4]$ at pH 3.0. The spectrum is a composite of three contiguous spectral windows.

When an oxalic acid solution is used to dissolve precipitated $[Pt(OH)_2]\cdot nH_2O$, new resonances are observed at −24 and −338 ppm at the expense of **6**. The smaller peak, at −24 ppm, is consistent with monodentate carboxylato substitution for H_2O.[29] This resonance is assigned to the monodentate $[Pt(OxH\text{-}O)(H_2O)]_3^+$ (**7**). The dominant peak in the spectrum is at −338 ppm. The large upfield shift of this resonance from **6** and **7** is consistent with the formation of bidentate $[Pt(Ox)(H_2O)_2]$ (**8**). As the reaction progresses, the resonance at −338 ppm is replaced by a peak at −525 ppm, consistent with the formation of **5** as discussed previously. A small peak is also observed at −345 ppm. The small shift of this peak from that of **8** indicates a complex with one oxalate ligand bidentate and the other monodentate. The complex is assigned as $[Pt(Ox)(OxH\text{-}O)(H_2O)^-]$ (**9**).

When these solutions are exposed to air, dark blue colors are observed, followed by broadening and disappearance of the resonance for **5**. When these solutions are heated between 20 and 60 °C, the line width at half-height changes from 1000 to 200 Hz at the same time as the color of the solution changes from dark blue to light green. When blue solutions are diluted with H_2O, the line width at half-height changes from 1000 to 200 Hz as the color of the solutions change from blue, to green, to yellow. When alkali-metal salts are added to acidic blue solutions, copper-colored needles rapidly precipitate from solution. These observations are consistent with reports of polymerization of air-oxidized concentrated solutions of **5**.[14,43]

Malonate Reactions. When malonic acid is added to a solution of **1** and the pH of the solution is adjusted to 3.0, new resonances are observed in the ^{195}Pt spectrum, as shown in Figure 1.

A small peak is observed at −1149 ppm, which is 36 ppm to lower field than $[PtCl_3(H_2O)]^-$.[29] This shift is consistent with replacement of coordinated H_2O with a monodentate carboxylato ligand and is assigned to the monodentate malonato complex $[Pt(MalH\text{-}O)Cl_3]^{2-}$ (**10**). The dominant peak in the ^{195}Pt spectrum is at −978 ppm, 167 ppm to higher shielding than the peak of the cis isomer of $[PtCl_2(H_2O)_2]$.[27] The ^{13}C NMR spectrum of a solution containing 90% of this complex shows a single resonance in the carboxyl region at 179.47 ppm. This is consistent with a bidentate malonato complex, with equivalent carboxylato groups. This peak is assigned to the bidentate malonato species $[PtCl_2(Mal)]^{2-}$ (**11**). Two small peaks are observed at −595 and −562 ppm. These resonances become dominant species at equilibrium in the ^{195}Pt NMR spectrum at pH 6.0. Concentration of these solutions causes precipitation of a yellow solid. When this solid is isolated and dissolved in H_2O, a single resonance is observed at −562 ppm. The ^{13}C NMR spectrum shows a single resonance in the carboxyl region at 180.36 ppm. The resonance at −562 ppm is assigned to the bis(malonato) complex with both malonates bidentate, $[Pt(Mal)_2]^{2-}$ (**13**). The resonance at −595 ppm loses intensity as the resonance for **13** increases, and the resonance at −595 ppm is the predominant resonance in the supernate after isolating **13**. The resonance at −595 ppm is consistent with the chloro bis(malonato) complex $[Pt(Mal)(MalH\text{-}O)Cl]^{2-}$ (**12**), with one malonate bidentate and the other malonate monodentate. Integratable ^{13}C and ^{195}Pt NMR spectra of the reaction of **13** with KCl are shown in Figure 2. The ^{13}C spectrum reveals four resonances for different carboxyl carbons of equal intensity, shifted from the overlapping resonances of **11** and **13**, and the free malonic acid resonance. The four resonances are in agreement with four nonequivalent carboxyl groups in **12**.

When malonic acid is used to dissolve the neutral solid $[Pt(OH)_2]\cdot nH_2O$, new resonances are observed to form at the expense of **6**, as shown in Figure 3.

A new resonance is observed at −32 ppm. The small shift from the resonance of **5** indicates that the new species is formed by replacement of H_2O with monodentate carboxylate. This resonance is assigned to $[Pt(MalH\text{-}O)(H_2O)_3]^+$ (**14**). Subsequently, a peak is observed at −314 ppm. The large upfield shift of this resonance from **6** and **14** is consistent with the formation of the bidentate complex $Pt(Mal)(H_2O)_2$ (**16**). Two other resonances are observed at −74 and −331 ppm. The small shift of the resonance at −74 ppm from the resonance of **14** is consistent with the formation of a bis(malonato) complex with both malonates monodentate. Cis or trans geometry cannot be established from the NMR spectrum; however, the structure of the complex can

(43) Papavassiliou, G. C. *J. Phys. C.* **1977**, *10*, 489.

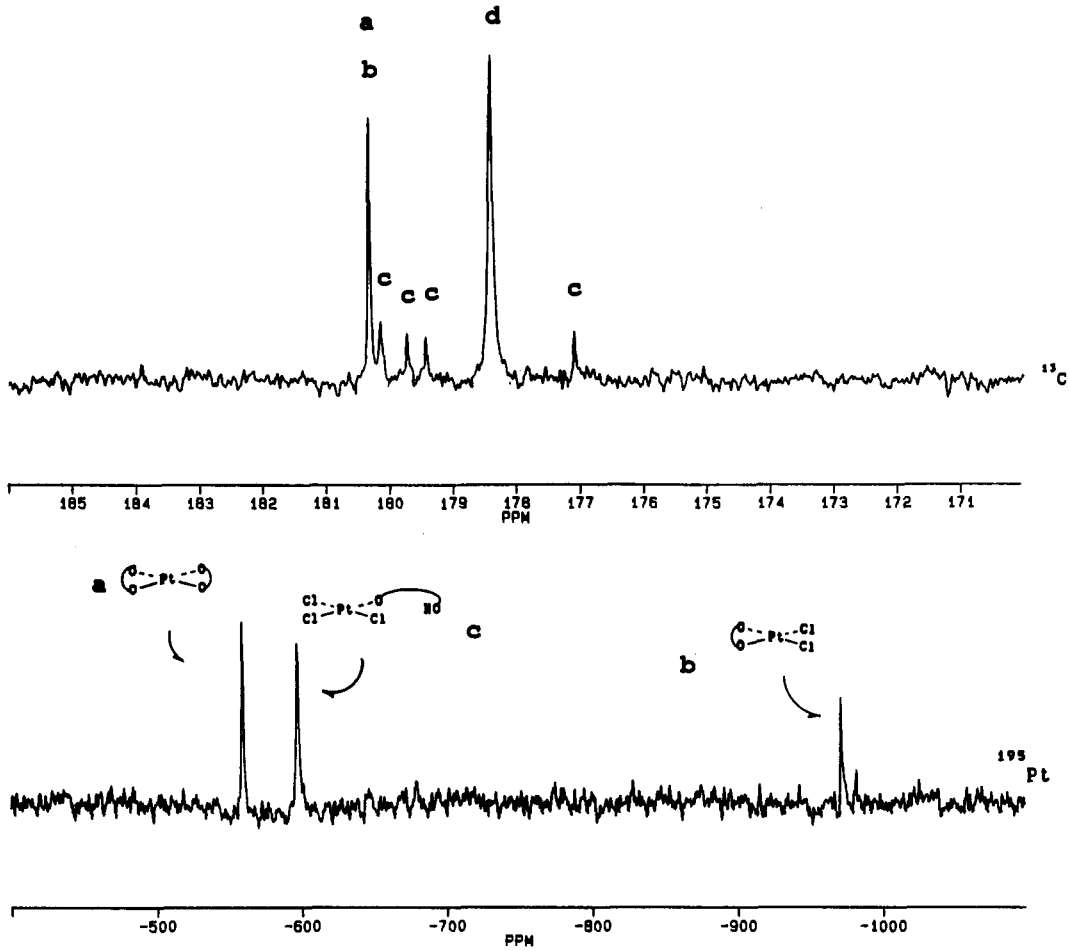

Figure 2. ^{13}C and ^{195}Pt NMR spectra of the reaction of $[Pt(Mal)_2]^{2-}$ with KCl: top, ^{13}C spectrum of the carboxylate region; bottom, ^{195}Pt spectrum of the Pt(II) malonato region. a = $[Pt(Mal)_2]^{2-}$; b = $[Pt(Mal)Cl_2]^{2-}$; c = $[Pt(Mal)(MalH\text{-}O)Cl]^{2-}$; d = $MalH_2$. Mal = malonato.

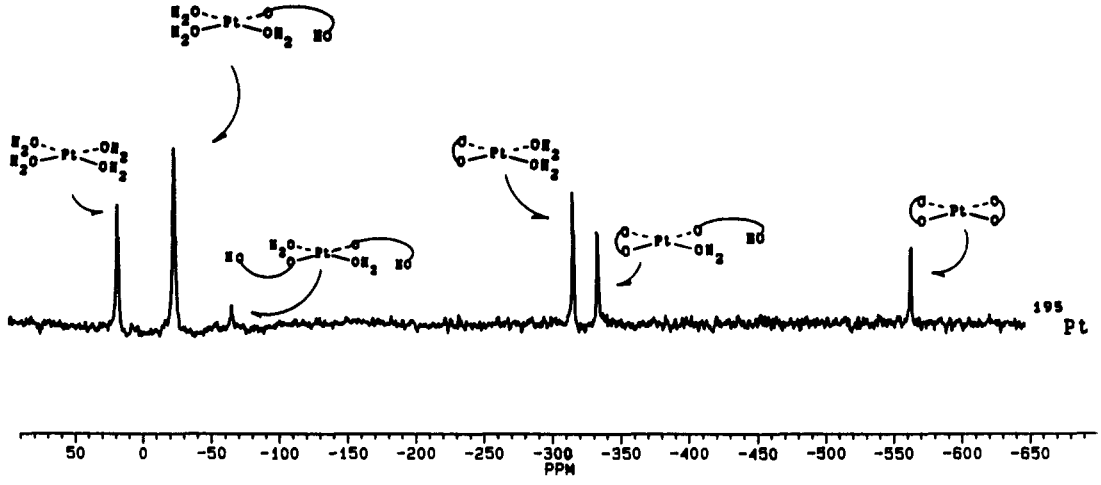

Figure 3. ^{195}Pt NMR spectrum of the reaction of malonic acid with $[Pt(OH)_2]\cdot nH_2O$ at pH 1.5. The spectrum is a composite of two contiguous spectral windows taken 12 h (downfield) and 48 h (upfield) after starting the reaction.

be rationalized on the basis of the trans effect and chelate ring formation. The bis complex with two monodentate carboxylato groups is only observed for reactions of $MalH_2$ and $MmalH_2$ with **6**. A second carboxylato group added to **14** should be directed trans to the first because carboxylate is a better trans director than water. However, *cis*- and *trans*-bis(carboxylato) species have been observed for the reaction of glycine and **6**.[29] The pH of these reactions was 1.5 so that the amine nitrogen of glycine was protonated. Kinetically, glycine chelate ring closure could be much slower than for the monodentate carboxylato species described here. The absence of cis bis monodentate species under our reaction conditions can then be accounted for by carboxylate being a better trans director than water and fast chelate ring closure of any cis bis species. In the reactions of $MalH_2$ and $MmalH_2$ with **1**, chelate ring closure of a monodentate species would be favored over formation of cis or trans bis monodentate complexes because chloride is a better trans director than carboxylate. We assign the peak to *trans*-$[Pt(MalH\text{-}O)_2(H_2O)_2]$ (**15**) with both malonates monodentate.

Another resonance is observed at −331 ppm. The small shift of this resonance from that of **16** is consistent with the formation of a bis(malonato) complex with one malonate bidentate and the other malonate monodentate. The resonance is assigned to the complex $[Pt(Mal)(MalH\text{-}O)(H_2O)]^-$ (**17**). The resonance for **13**

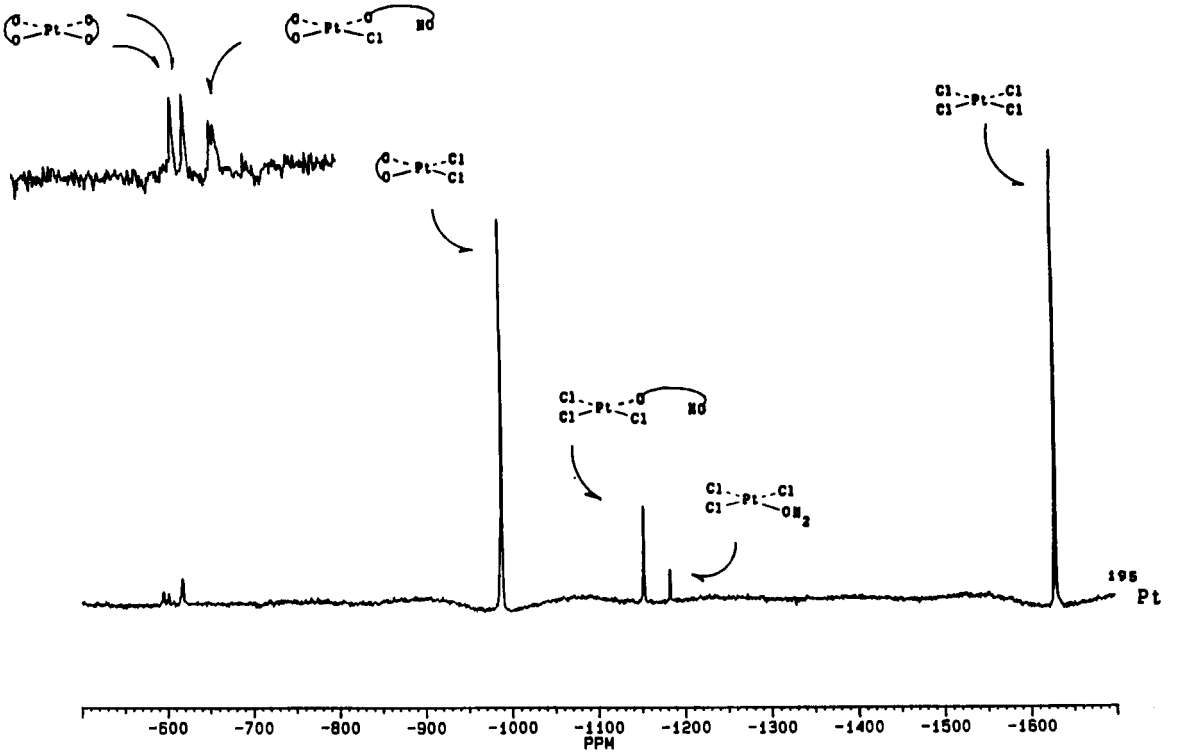

Figure 4. ^{195}Pt NMR spectrum of the reaction of 2-methylmalonic acid with $K_2[PtCl_4]$ at pH 3.0. The spectrum is a result of three contiguous spectral windows. Upper inset: detail of the bis(2-methylmalonato) region of the ^{195}Pt spectrum at pH 6.0.

at −562 ppm is observed to increase in concentration as the reaction progresses.

2-Methylmalonate Reactions. Figure 4 is a ^{195}Pt NMR spectrum observed when 2-methylmalonic acid is added to a solution of **1** at pH 3.0. A new resonance is observed at −1149 ppm. Again, the proximity of this resonance to that of $[PtCl_3(H_2O)]^-$[29] is consistent with replacement of coordinated H_2O with a carboxylato group, and this resonance is assigned to the monodentate 2-methylmalonato complex $[Pt(MmalH\text{-}O)Cl_3]^{2-}$ (**18**). The dominant peak in the ^{195}Pt spectrum is at −995 ppm, 184 ppm to higher field than that of *cis*-$[PtCl_2(H_2O)_2]$.[29] The ^{13}C spectrum of a solution containing 90% of this complex shows a single dominant resonance in the carboxyl region at 181.43 ppm, consistent with a bidentate 2-methylmalonato species. This resonance is assigned to the bidentate 2-methylmalonato species $[Pt(Mmal)Cl_2]^{2-}$ (**19**).

In low-digital-resolution ^{195}Pt NMR spectra, three small peaks are observed at −623, −608, and −600 ppm at pH 3.0 and greater. These peaks become dominant when solutions of pH 6.0 are allowed to reach equilibrium. At higher digital resolution, the resonance at −623 ppm is observed to be two peaks of equal intensity separated by 0.5 ppm. The resonances at −623 ppm arise from two diastereomers of $[Pt(Mmal)(MmalH\text{-}O)Cl]^{2-}$ (**20**, **21**), in which one of the ligands is bidentate and the other monodentate. The two resonances result from an interesting form of diastereomerism arising from the fact that both α-carbon atoms are chiral in a complex like **20**, shown in Chart I. The two chiral centers result in two diastereomeric pairs of enantiomers for **20** and **21**. Thus, the observation of two ^{195}Pt resonances at −623 ppm affords further evidence for monodentate, bidentate structures.

Concentration of these solutions gives a yellow solid. When this solid is isolated and dissolved in H_2O, two ^{195}Pt resonances are observed at −608 and −600 ppm. These peaks are consistent with formation of two different isomers of bidentate bis(2-methylmalonato)platinate(II) as shown in Chart I. We have drawn the chelate rings in an idealized planar geometry, which makes it apparent that one isomer has methyl groups in a syn orientation with respect to the coordination plane of Pt (**22**) and the other isomer has methyl groups in an anti orientation (**23**). Other workers have shown that Pt(II) complexes with malonato chelate rings prefer a boat conformation in the solid state.[22,23]

Chart I. Idealized Structures of 2-Methylmalonato Complexes

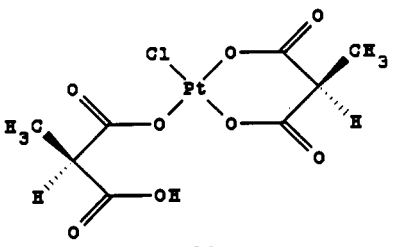

20

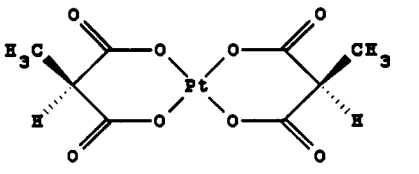

22

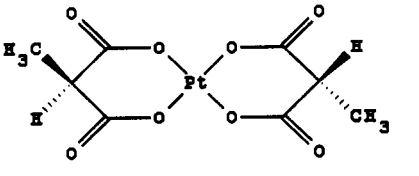

23

Several conformations of this chelate ring have similar energies and can be observed in solution. The solubilities of the syn and anti isomers are different. When the yellow solid is extracted with cold water, the ^{195}Pt, ^1H, and ^{13}C NMR spectra show resonances of unequal intensity for the two isomers. When undissolved solid is added to cold water extractions, the ^{195}Pt NMR resonance at −600 ppm (^1H: 4.1 (q), 1.13 ppm (d)) increases in intensity. The structure of the least soluble isomer was shown by X-ray crystallography (vide infra) to be potassium *anti*-bis(2-methylmalonato)platinate dihydrate (**23**). Therefore, the more soluble isomer whose ^{195}Pt resonance is at −608 ppm (^1H: 4.15 (q), 1.10

Scheme I. Reactions of Pt(II) with Dicarboxylic Acids

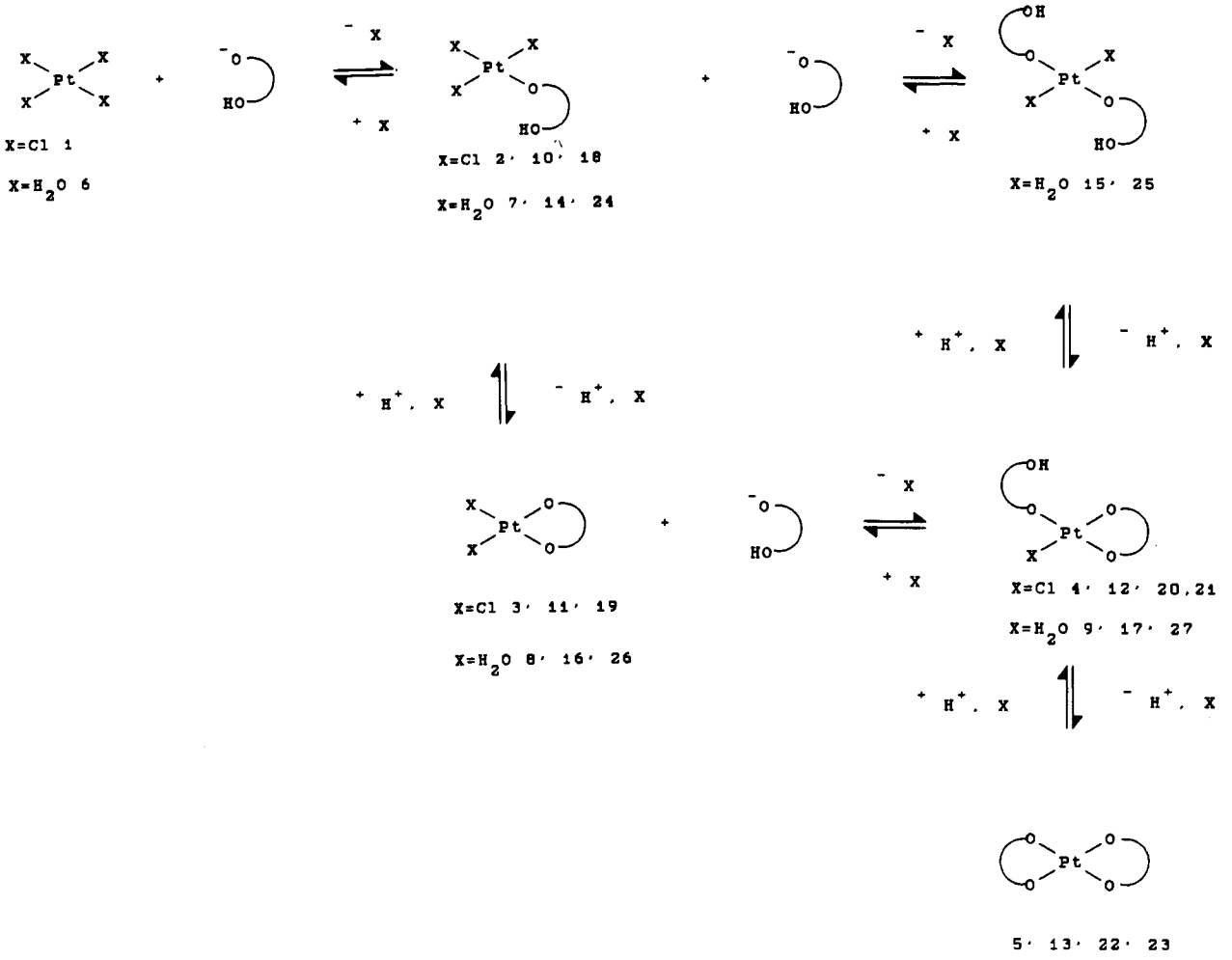

ppm (d)) is the *syn*-bis(2-methylmalonato)platinate(2−) complex (**22**). The ^1H spectra reveal a temperature dependence for the syn isomer **22**. Between 0 and 60 °C, the methine resonance for **22** shifts 0.18 ppm downfield, while the proton resonances of the anti isomer **23** are only slightly temperature dependent (0.03 ppm). The methine resonance for **23** is upfield from that of **22**, while the methyl resonance for **23** is downfield from that of **22**. This is as expected from the crystal structure, in which it is observed that the methine protons of **23** lie in the shielding cone of the carbonyl group, while the methyl protons in the plane of the carbonyl group are deshielded. The equivalence of the protons for **22** shows that ring conformations are in rapid equilibrium on the NMR time scale. The temperature dependence of the resonances of **22** suggests that several ring conformers are differentially populated over the temperature range studied.

When 2-methylmalonic acid is added to the neutral solid $[Pt(OH)_2]\cdot nH_2O$, new resonances are observed to form at the expense of $[Pt(H_2O)_4]^{2+}$ (**6**). A peak is observed at −34 ppm. The small shift from the resonance of **6** indicates that the new species is formed by replacement of H_2O by a carboxylato group. This resonance is assigned to $[Pt(MmalH\text{-}O)(H_2O)_3]^+$ (**24**). The next peak that is observed is at −339 ppm. The large shift of this resonance from those of **6** and **24** is consistent with the formation of the bidentate complex $[Pt(Mmal)(H_2O)_2]$ (**26**). Small single resonances are also observed at −78 and −356 ppm. The small shift of the resonance at −78 ppm from that of **24** is consistent with the formation of a bis(2-methylmalonato) complex with both 2-methylmalonate ligands monodentate. We predict that the carboxylato groups have trans geometry about the Pt, as previously described for the analogous bis(malonato) complex **15**. The resonance is assigned to *trans*-$[Pt(MmalH\text{-}O)_2(H_2O)_2]$ (**25**). The small shift of the peak at −356 ppm from that of **26** is consistent with a complex having one 2-methylmalonato ligand bidentate and the other 2-methylmalonato ligand monodentate. The resonance is assigned to the complex $[Pt(Mmal)(MmalH\text{-}O)(H_2O)]^-$ (**27**). The remaining peaks that are observed are at −600 and −608 ppm. These resonances correspond to the bis bidentate complexes **23** and **22** discussed above.

Table VI. $K_2[Pt(C_2O_4)Cl_2]\cdot H_2O$: Bond Lengths (Å) and Angles (deg) with Standard Deviations for all Non-Hydrogen Atoms

Bond Lengths			
Pt–Cl(1)	2.298 (4)	Pt–Cl(2)	2.291 (3)
Pt–O(2)	2.04 (1)	Pt–O(1)	2.03 (1)
O(3)–C(1)	1.23 (2)	O(2)–C(2)	1.28 (2)
O(1)–C(1)	1.28 (2)	O(4)–C(2)	1.22 (2)
C(1)–C(2)	1.59 (2)		

Bond Angles			
Cl(1)–Pt–Cl(2)	93.0 (1)	Cl(1)–Pt–O(2)	174.7 (2)
Cl(2)–Pt–O(2)	92.3 (2)	Cl(1)–Pt–O(1)	91.9 (3)
Cl(2)–Pt–O(1)	174.9 (3)	O(2)–Pt–O(1)	82.8 (4)
Pt–O(2)–C(2)	113 (1)	Pt–O(1)–C(1)	113 (1)
O(3)–C(1)–O(1)	126 (1)	O(3)–C(1)–C(2)	119 (1)
O(1)–C(1)–C(2)	116 (1)	O(2)–C(2)–O(4)	125 (1)
O(2)–C(2)–C(1)	115 (1)	O(4)–C(2)–C(1)	121 (1)

Crystallographic Studies. $K_2[Pt(C_2O_4)Cl_2]\cdot H_2O$ (3). The structure of the anionic complex of **3** is shown in Figure 5, and bond distances and angles are given in Table VI. Bond lengths and angles are comparable to other known Pt–oxalate structures.[15,23,41] An interesting feature of the crystal structure is the zigzag-chain structure of the anionic units. The chloride of one complex is positioned above the oxalate carbonyl carbon of the adjacent complex, resulting in an electrostatistically favored conformation. The Pt–Pt separations of 3.799 (2) Å between Pt's in the same unit cell and 3.815 (2) Å between Pt's in adjacent unit cells suggest minimal Pt–Pt interaction.

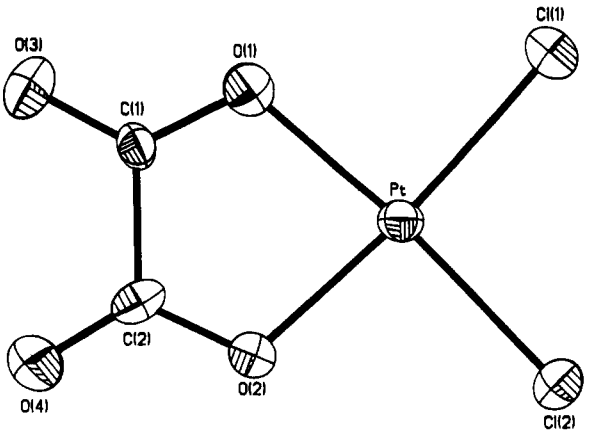

Figure 5. Thermal ellipsoid plot of $[Pt(C_2O_4)Cl_2]^{2-}$ showing 50% probability ellipsoids and numbering scheme for the structure.

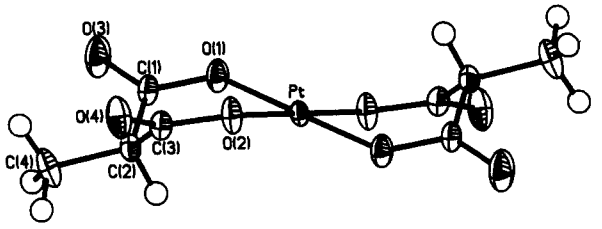

Figure 6. Thermal ellipsoid plot of $[anti\text{-}Pt(C_4H_4O_4)_2]^{2-}$ showing 50% probability ellipsoids and numbering scheme for the structure.

Table VII. $K_2[anti\text{-}Pt(C_4H_4O_4)_2]\cdot 2H_2O$: Bond Lengths (Å) and Angles (deg) with Standard Deviations for all Non-Hydrogen Atoms

Bond Lengths			
Pt–O(1)	2.010 (4)	Pt–O(2)	2.000 (4)
O(1)–C(1)	1.301 (6)	O(2)–C(3)	1.290 (6)
C(1)–C(2)	1.519 (7)	C(1)–O(3)	1.226 (8)
C(2)–C(3)	1.537 (7)	C(2)–C(4)	1.518 (7)
C(3)–O(4)	1.228 (8)		
Bond Angles			
O(1)–Pt–O(2)	92.5 (2)	Pt–O(1)–C(1)	121.0 (4)
Pt–O(2)–C(3)	122.1 (3)	O(1)–C(1)–C(2)	118.4 (5)
O(1)–C(1)–O(3)	120.7 (5)	C(2)–C(1)–O(3)	120.9 (5)
C(1)–C(2)–C(3)	111.6 (3)	C(1)–C(2)–C(4)	113.3 (5)
C(3)–C(2)–C(4)	112.0 (5)	O(2)–C(3)–C(2)	117.9 (5)
O(2)–C(3)–O(4)	121.6 (5)	C(2)–C(3)–O(4)	120.4 (4)

$K_2[anti\text{-}Pt(C_4O_4H_4)_2]\cdot 2H_2O$ (23). The structure of the anionic complex of **23** is shown in Figure 6, and bond distances and angles are listed in Table VII. Crystallographic studies on malonato and other substituted malonato Pt complexes are in agreement with the bond length and bond angle determinations we have made for **23**.[20,21] The 2-methylmalonato ligand is in a boat conformation, as is the case with other Pt(II) malonate derivatives. The anionic units also stack in a columnar chain along the crystallographic *a* axis. The long Pt–Pt distance of 4.059 (2) Å suggests no interaction between metal centers. Hydrogen-bonding interactions between pairs of lattice waters and the O(4) atoms of neighboring anionic units (each water hydrogen-bonded to two O(4) atoms and each O(4) to two waters in a diamond pattern) link neighboring "columns" of anionic units in chains that run along the unit cell *a,c* diagonal. The potassium ion is seven-coordinated in **23**, while in **3** K(1) and K(2) are eight- and seven-coordinated, respectively. If there is hydrogen bonding to the lattice water in **3**, it is very weak (nearest O···O contact is 3.00 Å).

Summary

Our investigation of multidentate oxygen-bound ligands by ^{195}Pt and ^{13}C NMR spectroscopy and X-ray crystallography shows that a complex equilibrium exists between monodentate and bidentate Pt(II) complexes that can be described by Scheme I. The reactions are dependent upon pH and the ligand, X^-. NMR spectra provide direct evidence for monodentate complexes in high concentrations during formation reactions and in low concentrations at equilibrium. Complexes have been characterized by X-ray diffraction, and intermediate species have been identified by their solution NMR spectra.

Acknowledgment. We gratefully acknowledge support for this work from a Local Institutional grant from the American Cancer Society (IN 172) and grants from the National Science Foundation, the National Institutes of Health, and the M. J. Murdock Charitable Trust. We are also grateful for a generous loan of platinum from the Johnson Matthey Corp.

Registry No. **1**, 10025-99-7; **2**, 136426-20-5; **3**, 136426-21-6; **3**·H_2O, 136426-42-1; $(Bu_4N)_2$(**3**), 96240-99-2; **4**, 136426-22-7; **5**, 35371-78-9; $(Bu_4N)_2$(**5**), 87134-19-8; **7**, 136426-23-8; **8**, 136426-24-9; **9**, 136426-25-0; **10**, 136426-26-1; **11**, 136426-27-2; **12**, 136426-28-3; K_2(**13**), 52241-24-4; Na_2(**13**), 136426-29-4; $(Bu_4N)_2$(**13**), 136426-43-2; **14**, 136426-30-7; **15**, 136426-31-8; **16**, 136426-32-9; **17**, 136426-33-0; **18**, 136426-34-1; **19**, 136426-35-2; **20**, 136426-36-3; K_2(**22**), 136426-37-4; Na_2(**22**), 136521-27-2; $(Bu_4N)_2$(**22**), 136521-30-7; K_2(**23**), 136597-71-2; Na_2(**23**), 136521-28-3; K_2(**23**)·H_2O, 136597-72-3; $(Bu_4N)_2$(**23**), 136597-74-5; **24**, 136426-38-5; **25**, 136426-39-6; **26**, 136426-40-9; **27**, 136426-41-0; ^{195}Pt, 14191-88-9.

Supplementary Material Available: Listings of crystal data and structure refinement parameters, anisotropic thermal parameters, calculated H atom coordinates, least-squares planes, and potassium coordination and lattice water contacts and packing diagrams (3 pages); listings of observed and calculated structure factors (42 pages). Ordering information is given on any current masthead page.